

# Secondary Control for Cyber-Physical Interconnected Microgrid Systems

**Ngoc An Luu**

University of Da Nang - University of Science and Technology, Vietnam  
lnan@dut.udn.vn (corresponding author)

**Tung Lam Nguyen**

University of Da Nang - University of Science and Technology, Vietnam  
ntlam@dut.udn.vn

Received: 24 January 2025 | Revised: 18 February 2025 | Accepted: 28 February 2025

Licensed under a CC-BY 4.0 license | Copyright (c) by the authors | DOI: <https://doi.org/10.48084/etasr.10333>

## ABSTRACT

**This paper presents a comprehensive analysis of the design, control frameworks, and practical implementation of interconnected microgrids, with an emphasis on improving system resilience and reliability. To overcome architectural challenges, a hierarchically distributed control system is proposed, featuring both microgrid-level and system-wide control layers. A multi-agent system is employed to oversee control elements in each microgrid and to facilitate cooperation with neighboring grids. Additionally, the paper introduces a Cyber Hardware-in-the-Loop (CHIL) framework, designed to function as a real-time simulation platform for the cyber-physical aspects of these systems, integrating network emulation, real-time power system dynamics, and multiagent control coordination.**

*Keywords-microgrid; distributed control; cyber hardware-in-the-loop; cyber-physical system; real-time*

## I. INTRODUCTION

Microgrids (MGs) play a vital role in the future of power systems, offering a decentralized model for energy generation, distribution, and management. Unlike conventional centralized grids, MGs can operate in both grid-connected and islanded modes, enabling increased flexibility. This dual operational capability enhances resilience and system efficiency while supporting the integration of renewable energy sources, making MGs a crucial innovation in modern power infrastructure.

However, managing interconnected MG systems presents new challenges compared to isolated ones. The increased complexity due to interconnected electrical and communication infrastructures requires advanced control systems. Several studies have focused on extending single MG control schemes to interconnected MGs [1-4]. For instance, in [1], a two-layer distributed hierarchical control scheme was introduced for AC-connected MGs, which was expanded in [2] for DC microgrid clusters. Other studies, such as [3, 4], investigated control mechanisms such as droop-based regulation for small signal stability in PV-based MG clusters and consensus control for multiple MGs. However, these studies often lack higher-level coordination for optimized system dispatch, and limited access to data due to privacy concerns makes a distributed control architecture with minimal data sharing highly desirable.

This paper examines the structure, distributed hierarchical control, and implementation of interconnected MGs within a cyber-physical framework, incorporating both loads and

various Distributed Energy Resources (DERs). The control system is carefully designed to manage multiple tasks across different layers and time scales. At the primary level, control systems link the local DERs' management to the network-level coordination of interconnected MGs. Secondary control ensures the stabilization of frequency and voltage around reference points while facilitating balanced power distribution. Finally, tertiary control focuses on achieving overall system optimization. A Multi-Agent System (MAS) serves as the test case for implementing distributed control within a peer-to-peer communication network. The MAS oversees the components of individual MGs and coordinates with neighboring grids. In real-time applications, the MAS operates as a group of entities, each located in a different physical location and exchanging information via a communication network [5-8]. Each agent represents a specialized software program running on processors, such as Programmable Logic Controllers (PLCs) or microcontrollers, each fulfilling specific control tasks.

Implementing a MAS in a cyber-physical network of MGs introduces unique challenges, especially for practical deployment. To address these challenges, this paper introduces a real-time cyber-physical simulation platform called Cyber Hardware-in-the-Loop (CHIL). This platform simulates multi-domain systems by integrating network emulation, real-time power system simulation, and agent-based control. The CHIL setup operates asynchronously, reflecting real-world system operation, and the use of container-based agents allows the platform to be scalable, flexible, and reusable.

The main contributions of this study are:

- Fully distributed hierarchical control: Unlike conventional methods, this approach integrates multilayered control with consensus-based secondary control, ensuring accurate frequency, voltage, and power-sharing across MGs.
- Multi-agent system for decentralized coordination: The MAS allows peer-to-peer communication, eliminating the need for centralized control, enhancing scalability and improving system resilience.
- Cyber hardware-in-the-loop validation: A real-time CHIL testbed integrates OPAL-RT, ns-3 network emulation, and Docker-based agents, providing a comprehensive validation of both power system and communication dynamics.

## II. SYSTEM DESCRIPTION AND CONTROL SCHEMES

The interconnected MG system represents a sophisticated cyber-physical network, integrating both electrical and communication components. It can function either in islanded mode or connected to the main grid [9-11]. This research focuses on an islanded system of interconnected MGs that operate independently from the central grid. Each MG consists of clusters of dispatchable Distributed Generators (DGs) and local loads, all connecting at a common coupling point. These microgrids are linked via low-voltage to medium-voltage transformers, which tie each MG to a specific bus in the medium-voltage grid.

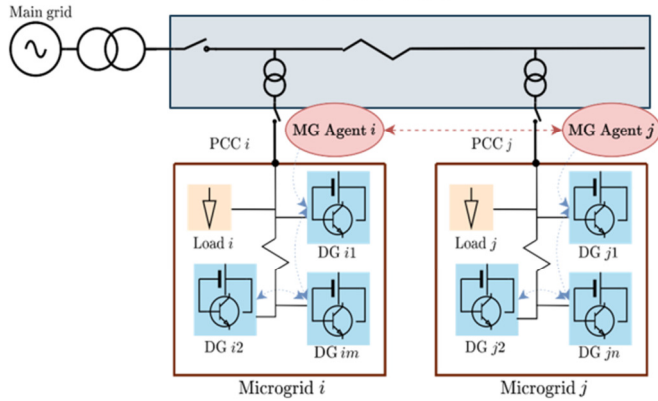


Fig. 1. Architecture of the interconnected MG systems with network communication.

The communication network within the interconnected MG system is organized hierarchically, with an upper-level network facilitating communication between MGs and a lower-level network connecting DGs within each individual MG, as shown in Figure 1. In this setup, each microgrid agent collects tie-line data and shares it with neighboring agents to create reference signals for frequency and voltage. The Distributed Generators (DGs) then adjust their operations to follow these reference signals, utilizing the existing distributed secondary control system in place for each MG.

## III. HIERARCHICAL CONTROL OF INTERCONNECTED MGs

### A. DG level

For islanded AC microgrids, managing inverter-interfaced DGs as voltage source inverters is crucial. Beyond droop control, it is essential to implement internal control loops that regulate both current and voltage. Additionally, incorporating a virtual impedance loop helps achieve precise power-sharing among DG units. Droop control is widely recognized for its effectiveness in regulating both voltage and frequency in inverter-based DGs within islanded microgrids. The dynamic droop behavior for the  $i^{\text{th}}$  DG can be described as follows [4]:

$$\omega_i = \omega^* - K_i^P P_i^m \quad (1)$$

$$V_i = V^* - K_i^Q Q_i^m P_i^m \quad (2)$$

where  $\omega^*$  and  $V^*$  represent the nominal values for frequency and voltage. The  $K^P$  and  $K^Q$  coefficients are typically selected based on the DG's output power capacity. The actual measured active and reactive power outputs are represented by  $P^m$  and  $Q^m$ . Adjustments to the frequency  $\omega_i$  and voltage  $V_i$  are made through control signals sent from the secondary control system to restore the DG to its nominal operational values.

### B. Microgrid (MG) Level

Figure 2 shows the distributed MG control layer, which includes necessary information about both local and neighboring components. The secondary control layer's primary function is to monitor the reference signals produced by the higher-level coordination of interconnected MGs, ensuring accurate power distribution among the DG units within each individual MG. Various techniques for distributed secondary control have been extensively explored in previous studies, covering both linear and nonlinear control strategies. Building on methods presented in [12-15], a linear control scheme for restoring frequency and distributing real power is proposed for the  $i^{\text{th}}$  DG as follows [4]:

$$\omega_{DG_i} = \omega_{MG_k}^* - K_{DG_i}^P P_{DG_i} + \Omega_{DG_i} \quad (3a)$$

$$\begin{aligned} \dot{\Omega}_{DG_i} = & \sum_{j=1}^{N_{MG_k}} a_{ij}^k (\omega_{DG_j} - \omega_{DG_i}) + g_i^k (\omega_{MG_k} - \omega_{DG_i}) \\ & + \sum_{j=1}^{N_{MG_k}} a_{ij}^k (K_{DG_j}^P P_{DG_j} - K_{DG_i}^P P_{DG_i}) \end{aligned} \quad (3b)$$

Similarly, the linear control scheme for voltage regulation and reactive power sharing is as follows [4]:

$$V_{DG_i} = V_{MG_k}^* - K_{DG_i}^Q Q_{DG_i} + e_{DG_i} \quad (4a)$$

$$\begin{aligned} \dot{e}_{DG_i} = & \sum_{j=1}^{N_{MG_k}} a_{ij}^k (e_{DG_j} - e_{DG_i}) + g_i^k (V_{MG_k} - V_{DG_i}) \\ & + \sum_{j=1}^{N_{MG_k}} a_{ij}^k (K_{DG_j}^Q Q_{DG_j} - K_{DG_i}^Q Q_{DG_i}) \end{aligned} \quad (4b)$$

where  $\Omega_{DG_i}$  and  $e_{DG_i}$  are the control signals provided by the secondary control system. The parameter  $a_{ij}^k$  represents the communication coefficient between  $i$  and  $j$  DGs within MG  $k$ , where  $a_{ij}^k > 0$  indicates a communication link, otherwise

$a_{ij}^k = 0$ . The pinning gain  $g_i^k$  represents the relationship for DG  $i$  in MG  $k$ , where  $g_i^k > 0$  if DG  $i$  receives  $\omega_{MG_k}$  and  $V_{MG_k}$  directly, and  $g_i^k = 0$  otherwise. The total number of DGs in MG  $k$  is represented by  $N_{MG_k}$ . The reference values for frequency and voltage,  $\omega_{MG_k}$  and  $V_{MG_k}$ , are computed by the interconnected MG control system.

### C. Interconnected MGs Level

In interconnected MG systems, control hierarchies are classified based on their response time and infrastructure requirements, including communication capabilities [16-19]. Figure 2 illustrates the distributed structure of the two control layers. The primary control layer responds quickly to address any frequency or voltage deviations that occur due to minor disturbances. Secondary control is responsible for regulating the system's frequency, voltage, and power-sharing. Peer-to-peer communications enable this entire control framework for interconnected MG systems.

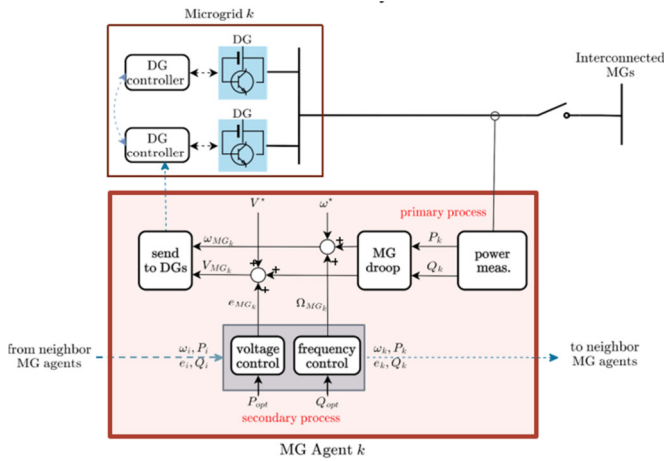


Fig. 2. Architecture of the interconnected MG systems with network communication.

#### 1) Primary Control Layer in Interconnected MGs

A droop control strategy, similar to the one used for DGs in a single MG, is employed for each MG to allow it to operate autonomously based on local measurements. The interconnected MG system consists of  $N$  buses, with the sets of buses, MGs, and lines denoted as  $N$ ,  $M$ , and  $V$ , respectively. The droop control for MG  $k$  can be defined as follows [4]:

$$\begin{aligned} \omega_{MG_k} &= \omega^* - K_k^P P_k, \quad k \in \mathcal{M} \\ V_{MG_k} &= V^* - K_k^Q Q_k, \quad k \in \mathcal{M} \end{aligned} \quad (6)$$

where  $\omega^*$  and  $V^*$  denote the nominal frequency and voltage amplitude at the interconnected MG level. The values  $P_k$  and  $Q_k$  represent the power exchanged between MG  $k$  and the interconnected system, while  $K_k^P$  and  $K_k^Q$  are the droop coefficients of each MG.

#### 2) Secondary Control Layer in Interconnected MGs

The distributed secondary control layer in interconnected MGs is designed to achieve three primary objectives:

1) restoring system frequency, 2) stabilizing the voltage at the Point of Common Coupling (PCC), and 3) maintaining optimal power-sharing among MGs. The secondary control laws for each MG can be formulated as follows [13]:

$$\omega_{MG_k} = \omega^* - K_k^P P_k + \Omega_{MG_k} \quad (7a)$$

$$\begin{aligned} \dot{\Omega}_{MG_k} &= \sum_{h=1}^M a_{kh} (\omega_h - \omega_k) + g_k (\omega^* - \omega_k) \\ &+ \sum_{h=1}^M a_{kh} [K_h^P (P_h - P_h^{opt}) - K_k^P (P_k - P_k^{opt})] \end{aligned} \quad (7b)$$

$$V_{MG_k} = V^* - K_k^Q Q_k + e_{MG_k} \quad (8a)$$

$$\begin{aligned} \dot{e}_{MG_k} &= (\sum_{h=1}^M a_{kh} (e_h - e_k) + (V^* - V^{PCC})) \\ &+ \sum_{h=1}^M a_{kh} \begin{pmatrix} K_h^Q (Q_h - Q_h^{opt}) \\ -K_k^Q (Q_k - Q_k^{opt}) \end{pmatrix} \quad k, h \in \mathcal{M} \end{aligned} \quad (8b)$$

In this system, the control signals  $\Omega_{MG_k}$  and  $e_{MG_k}$  are derived from secondary control within the interconnected MG system. The communication coefficient between MGs  $k$  and  $h$  is denoted by  $a_{kh}$ , while the pinning gain of MG  $k$  is represented by  $g_k$ . The total number of MGs is indicated by  $M$ .

The proposed control laws in (7) and (8) ensure that the interconnected MG system converges as follows [13]:

$$\lim_{t \rightarrow \infty} |\omega^* - \omega_k(t)| = 0 \quad (9)$$

$$\lim_{t \rightarrow \infty} |V^* - V^{PCC}(t)| = 0 \quad (10)$$

$$\lim_{t \rightarrow \infty} \begin{vmatrix} K_h^P (P_h(t) - P_h^{opt}) \\ -K_k^P (P_k(t) - P_k^{opt}) \end{vmatrix} = 0 \quad (11)$$

$$\lim_{t \rightarrow \infty} \begin{vmatrix} K_h^Q (Q_h(t) - Q_h^{opt}) \\ -K_k^Q (Q_k(t) - Q_k^{opt}) \end{vmatrix} = 0 \quad (12)$$

The distributed secondary control layer ensures that the system frequency at each bus in the interconnected MG system is restored to its reference value. Additionally, the voltage at the PCC is adjusted to match the reference value. The flow of real and reactive power is regulated according to the dispatch signals  $P_k^{opt}$  and  $Q_k^{opt}$ , which are provided by the optimal upper control layer. Any discrepancies caused by load changes are distributed among MGs based on their droop coefficients  $K_k^P$  and  $K_k^Q$ , as defined in (5) and (6) for each MG.

## IV. THE MULTIAGENT SYSTEM (MAS)

The distributed hierarchical control architecture introduced in this study utilizes a MAS that relies on peer-to-peer communication. An agent represents an autonomous entity that can collect local measurements, communicate with other agents, perform computations, and provide control signals to the DG-level controllers [20, 21]. Instead of relying on a centralized controller that aggregates data from the entire system, each agent processes only local and neighboring information. However, agents are capable of returning system-wide control signals to meet global objectives. Neighboring agents are identified based on the electrical connections in the interconnected MG system.

A. Agent

Agents are designed to function independently with limited system knowledge. Each agent is responsible for updating the power network state, performing necessary computations, and making control decisions. In the context of MGs, each agent's local controller implements droop control, using only local measurements, and acts as the primary control mechanism. To facilitate the proposed fully distributed multilayer control structure, agents are designed for practical system implementation. To simultaneously achieve all control objectives, each agent is equipped with two distinct processes that run in parallel. All participating MGs and their DGs collaborate to restore system-wide voltage and frequency. Under the distributed control scheme, MG agents exchange locally collected data to compute the consensus-based control laws described by (7) and (8). The process begins with agents collecting local measurements  $\omega_k, e_k, P_k, Q_k$  from the devices they are connected to. Next, they exchange messages  $\omega_k, e_k, K_k^P (P_k - P^{Ter}), K_k^Q (Q_k - Q^{Ter})$  with their neighbouring agents. These control signals are then calculated and sent to the relevant controllers. Finally, the reference frequency in the local controller is updated with the signal  $\Omega_k$ , and the reference voltage is adjusted using the signal  $e_k$ .

V. IMPLEMENTATION ON A REAL-TIME CYBER-PHYSICAL TESTBED

A. Experimental Setup

This section validates the agent design within the proposed control framework. The system under test is an interconnected MG composed of six buses operating in islanded mode. The test system includes three interconnected MGs: MG-1 and MG-2, each having three DGs, and MG-3 containing four DGs, as shown in Figure 3. The other buses in the system are assigned to loads. Figures 4 and 5 show the physical and cyber structure of the interconnected MG test system, where the communication network among agents mirrors the electrical connections at the MG level. Table I shows the parameters of the test interconnected system. The laboratory setup comprises two main components that are outlined in more detail below.

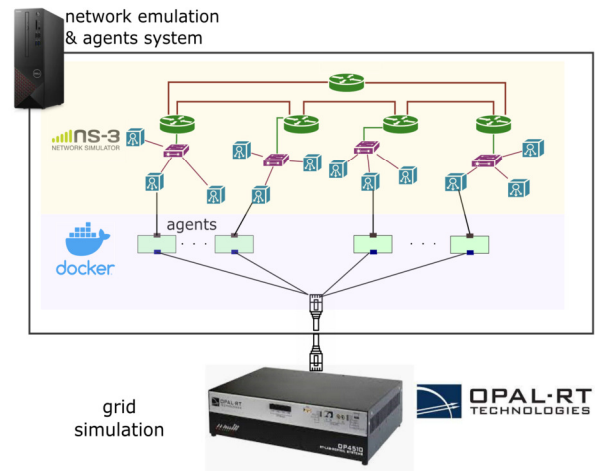


Fig. 4. Real-time Cyber-physical testbed configuration.

TABLE I. PARAMETERS OF THE TEST INTERCONNECTED SYSTEM

DGs	DG11-DG13	DG21-DG23	DG31-DG34
$K_{DG_i}^P \left( \frac{\text{Hz}}{\text{kW}} \right)$	3e-5	2e-5	4e-5
$K_{DG_i}^Q \left( \frac{\text{Hz}}{\text{kVAr}} \right)$	0.9e-5	0.6e-5	1.2e-5
Loads in interconnected MGs	Load 4	Load 5	Load 6
$P$ (kW)	15	15	15
$Q$ (kVAr)	10	6	8

1) Physical System

The physical system includes the electrical components of the interconnected MGs, along with the local DG controllers, simulated in real-time using the OPAL-RT simulator. Measurements from the MGs are sent to each agent, where the control signals  $\omega_{MGk}$  and  $V_{MGk}$  are computed and returned to the MG-level controllers within OPAL-RT. Communication between OPAL-RT and the agents is established using the User Datagram Protocol (UDP) as shown in Figure 4.

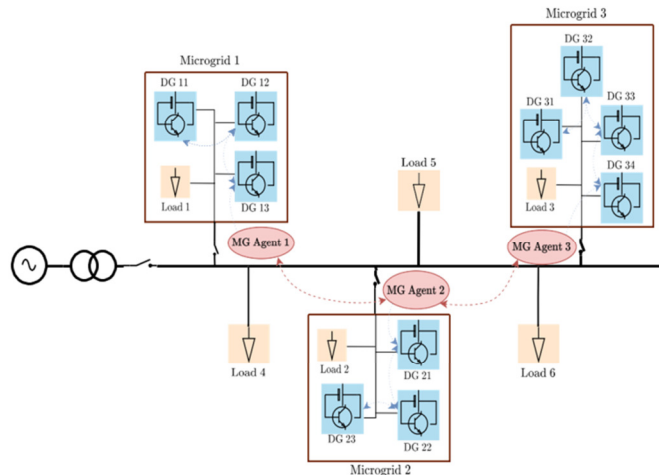


Fig. 3. Testbed configuration of the interconnected MG system.

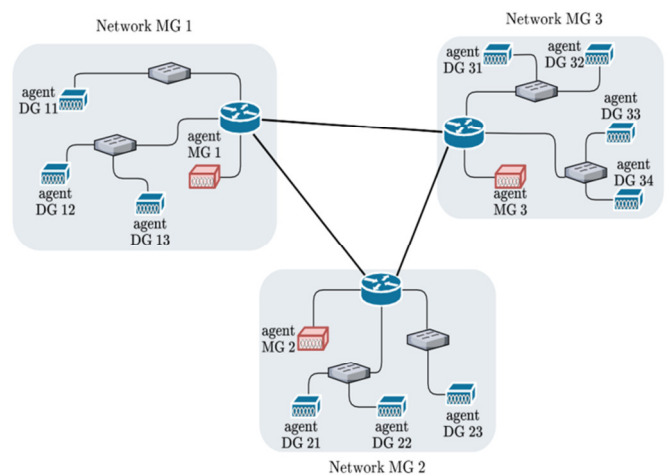


Fig. 5. Communication network topology.

## 2) Physical System

The cyber system runs on a Linux-based platform, utilizing Docker containers to implement the MAS and the network simulator ns3 as described in Figure 4.

### a) Network Emulation in NS3

The communication network topology of the interconnected MGs was emulated in ns3, a discrete-event simulator designed for communication networks, as shown in Figure 4. Each of the three local networks corresponds to one of the three MGs, and point-to-point connections facilitate communication between agents in different areas. Each agent is attached to an ns3 node to send and receive communication packets through the emulated network.

### b) Multi-Agent System in Docker Containers

The virtual network interface serves as a gateway for data exchange among containers, allowing interaction with the ns3 network emulation. This interface connects to Linux bridges, which link with the host operating system, using tapping devices to capture packets for user-space processing. These packets are then handled by ns3 through a custom net device, transmitting them to a designated ns3 ghost node. Meanwhile, the Real-time Publisher/Subscriber (RTPS) protocol in the DDS middleware facilitates communication between agents.

The Linux shared memory feature is employed to manage data sharing and interprocess communication. This setup allows multiple processes to concurrently access the same memory region, enhancing system efficiency. In this experiment, Docker containers and shared memory are used to create a buffer that serves two functions: (i) collecting measurement signals from OPAL-RT and transferring them to the container, and (ii) collecting control signals from the container and sending them back to OPAL-RT.

The distributed control algorithm is implemented by processing data collected from the power system simulation, combined with information exchanged over the communication network.

## B. Experimental Results

To validate the performance of the proposed control method, a 180-second Hardware-In-the-Loop (HIL) experiment was conducted. Data from the agents' logging and measurements stored in the simulator were analyzed to evaluate system behavior during the experiment. Two key moments in the experiment are  $t_1$  and  $t_2$ , corresponding to disturbances caused by changes in load power. The objectives of the experiment during a load step change in the interconnected MG system are as follows:

- The primary control computes the control inputs  $\Omega_{MGk}$  and  $e_{MGk}$  for the DG controllers in the MG, as described in (3) and (4).
- At the secondary control level, with a response time of several seconds, the system frequency is restored to the nominal value of 50 Hz. The PCC voltage of the interconnected MG system (bus 1) is adjusted to 1.00 p.u., while the voltage at other buses remains within upper and

lower limits. The DGs' real and reactive power outputs are distributed proportionally based on their rated capacities.

The real power, reactive power, frequency, and voltage profiles during the HIL experiment are illustrated in Figures 6, 7, 8, and 9, respectively.

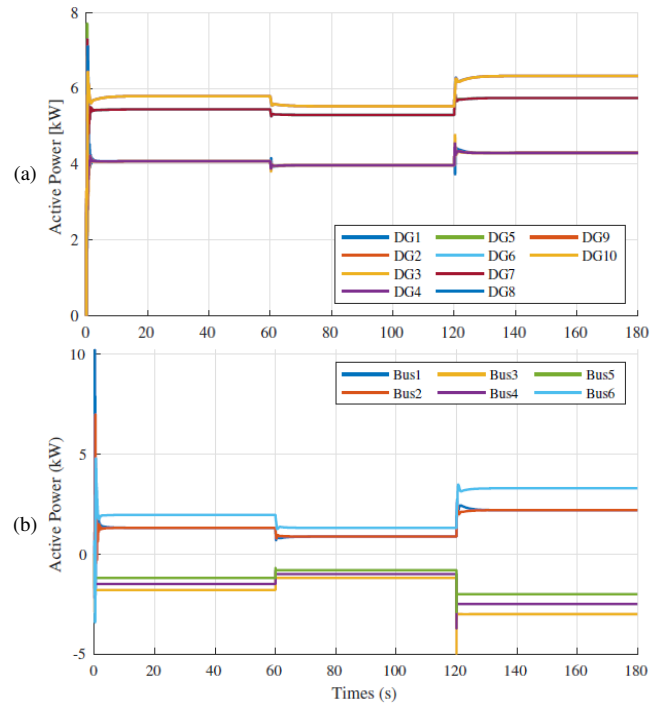


Fig. 6. Real power injections from (a) each DG and (b) bus in the interconnected MG system.

The results are presented in three time intervals:

For  $0 \leq t < t_1 = 60$ , OPAL-RT begins the simulation at  $t = 0$  s. As shown in Figures 6(a) and 7(a), the real and reactive power shared among DGs within each MG follows the respective DG droop coefficients. The measured frequencies are gradually restored to nominal values, as shown in Figure 8, and the PCC voltage at bus 1 is restored to 1 p.u in Figure 9(b).

For  $t_1 = 60 \leq t < t_2 = 120$ , the system experiences a load reduction at  $t_1 = 60$  s. Both frequency and voltage experience brief increases but are quickly restored to their reference values, thanks to the secondary control process. The power-sharing among DGs in each MG maintains the desired ratios.

For  $t_2 = 120 \leq t < t_3 = 180$ , an increase in load occurs at  $t_2 = 120$  s, causing the system frequency and bus voltage to drop. However, the agents' secondary control quickly restores both parameters to their reference values, ensuring that the power outputs of the DGs continue to follow the predefined sharing proportions.

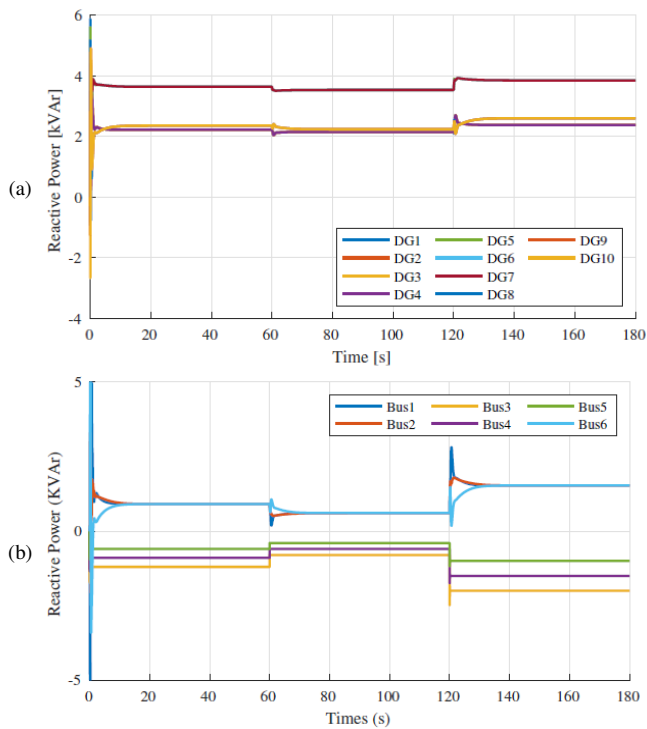


Fig. 7. Reactive power injections from (a) each DG and (b) bus in the interconnected MG system.

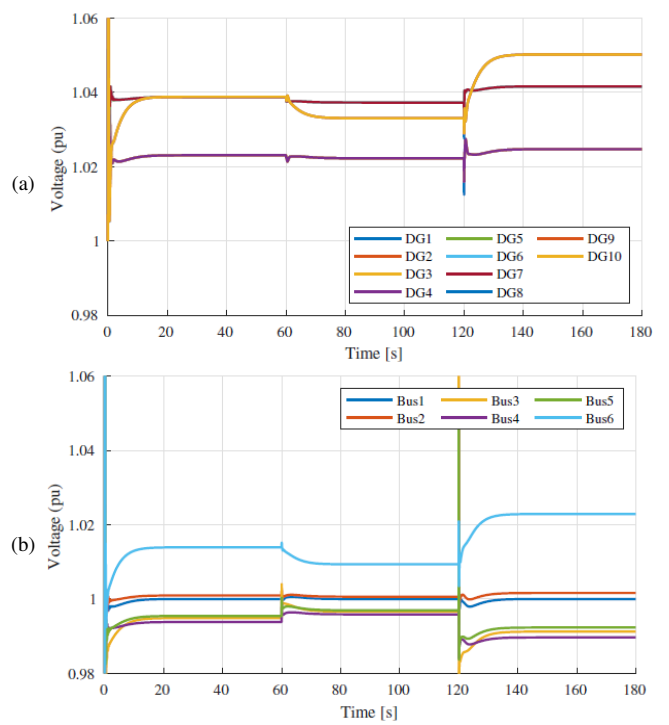


Fig. 9. Voltage of (a) each DG and (b) bus in the interconnected MG system.

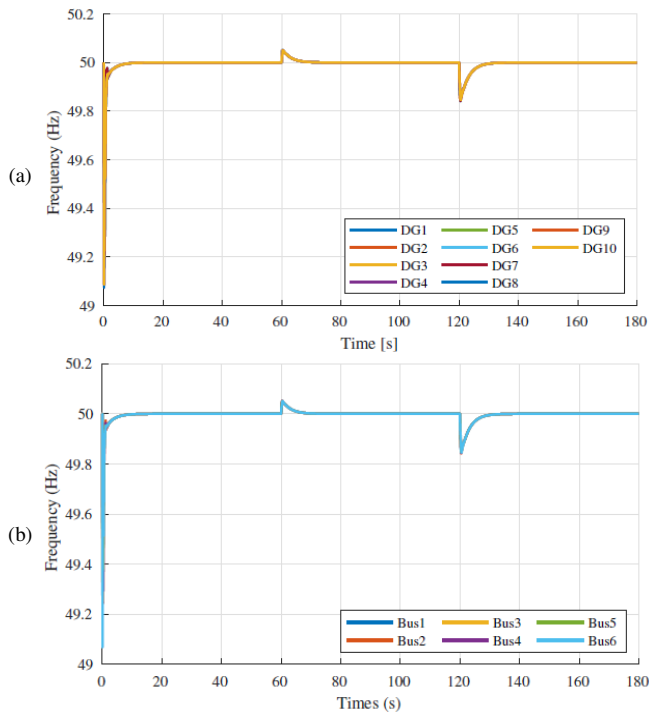


Fig. 8. Frequency for (a) each DG and (b) bus in the interconnected MG system.

C. Results' Discussion

The experimental results confirm that the proposed hierarchical distributed control framework effectively enhances the stability and coordination of interconnected MGs. The secondary control system successfully restores frequency and voltage to their nominal values after disturbances, ensuring system-wide stability. The results also demonstrate accurate power-sharing among DGs, maintaining proportional distribution based on droop coefficients. Unlike traditional centralized methods, the proposed MAS enables decentralized decision-making, reducing communication dependencies and improving fault resilience. The CHIL validation further highlights the system's ability to operate in real-time, accurately capturing the interaction between cyber and physical layers.

Additionally, the MAS-based control strategy minimizes communication delays while ensuring effective peer-to-peer coordination, as evidenced by the rapid response of DGs to dynamic load changes. The distributed nature of the control system allows seamless scalability, making it adaptable to various MG configurations. Experimental data confirm that the proposed framework not only improves frequency and voltage regulation but also enhances overall system robustness against uncertainties in power demand. These findings validate the practical feasibility of the approach and its potential for real-world deployment in modern smart grids.

VI. CONCLUSIONS

This paper presents a general architecture alongside a hierarchical distributed control system specifically designed for

such interconnected MG systems. The proposed control system operates in multiple layers and timescales, addressing both the local MG control level and the broader interconnected MG control level. A MAS is utilized to manage the control components within individual MGs and facilitate coordination with neighboring MGs. The CHIL setup, utilizing the container-based approach, is introduced as a real-time cyber-physical platform for simulating this multi-domain system. The successful implementation of the MAS and the control system validates the feasibility and efficiency of the proposed approach. Furthermore, this control architecture is adaptable and can be extended to support other types of MG, including DC and hybrid AC/DC microgrids. The MAS can also be further enhanced with additional features, such as fault detection and diagnostics, and has the potential to be applied to other cyber-physical systems.

## REFERENCES

- [1] X. Wu, X. Wu, Y. Xu, and J. He, "A Hierarchical Control Framework for Islanded Multi-Microgrid Systems," in *2018 IEEE Power & Energy Society General Meeting (PESGM)*, Portland, OR, USA, Aug. 2018, pp. 1–5, <https://doi.org/10.1109/PESGM.2018.8586235>.
- [2] Q. Shafiee, T. Dragičević, J. C. Vasquez, and J. M. Guerrero, "Hierarchical Control for Multiple DC-Microgrids Clusters," *IEEE Transactions on Energy Conversion*, vol. 29, no. 4, pp. 922–933, Sep. 2014, <https://doi.org/10.1109/TEC.2014.2362191>.
- [3] Z. Zhao, P. Yang, Y. Wang, Z. Xu, and J. M. Guerrero, "Dynamic Characteristics Analysis and Stabilization of PV-Based Multiple Microgrid Clusters," *IEEE Transactions on Smart Grid*, vol. 10, no. 1, pp. 805–818, Jan. 2019, <https://doi.org/10.1109/TSG.2017.2752640>.
- [4] Y. Wang *et al.*, "A Distributed Control Scheme of Microgrids in Energy Internet Paradigm and Its Multisite Implementation," *IEEE Transactions on Industrial Informatics*, vol. 17, no. 2, pp. 1141–1153, Oct. 2021, <https://doi.org/10.1109/TII.2020.2976830>.
- [5] T. L. Nguyen, Q. T. Tran, R. Caire, Y. Wang, Y. Besanger, and N. A. Luu, "Distributed optimal power flow and the multi-agent system for the realization in cyber-physical system," *Electric Power Systems Research*, vol. 192, Mar. 2021, Art. no. 107007, <https://doi.org/10.1016/j.epsr.2020.107007>.
- [6] C. Dou, Z. Zhang, D. Yue, and Y. Zheng, "MAS-Based Hierarchical Distributed Coordinate Control Strategy of Virtual Power Source Voltage in Low-Voltage Microgrid," *IEEE Access*, vol. 5, pp. 11381–11390, 2017, <https://doi.org/10.1109/ACCESS.2017.2717493>.
- [7] Y. Han, K. Zhang, H. Li, E. A. A. Coelho, and J. M. Guerrero, "MAS-Based Distributed Coordinated Control and Optimization in Microgrid and Microgrid Clusters: A Comprehensive Overview," *IEEE Transactions on Power Electronics*, vol. 33, no. 8, pp. 6488–6508, Dec. 2018, <https://doi.org/10.1109/TPEL.2017.2761438>.
- [8] M. Maaruf, S. El-Ferik, F. S. Al-Ismael, and M. Khalid, "A Decentralized Multiagent-Based Robust Backstepping Control for Restoring Secondary Voltage and Frequency of Autonomous Microgrids," in *2022 11th International Conference on Renewable Energy Research and Application (ICRERA)*, Istanbul, Turkey, Sep. 2022, pp. 430–435, <https://doi.org/10.1109/ICRERA55966.2022.9922805>.
- [9] S. Ahmad, S. Mekhilef, and H. Mokhlis, "An Intelligent Interconnection Module for Multiple Self-healed Interconnected Microgrids," in *2021 IEEE 4th International Conference on Computing, Power and Communication Technologies (GUCON)*, Kuala Lumpur, Malaysia, Sep. 2021, pp. 1–6, <https://doi.org/10.1109/GUCON50781.2021.9573958>.
- [10] D. Saha, N. Bazmohammadi, J. C. Vasquez, and J. M. Guerrero, "Multiple Microgrids: A Review of Architectures and Operation and Control Strategies," *Energies*, vol. 16, no. 2, Jan. 2023, Art. no. 600, <https://doi.org/10.3390/en16020600>.
- [11] P. Wu, W. Huang, N. Tai, J. Xie, and B. Lv, "An advanced architecture of multiple microgrids interfacing with UCC," in *2017 IEEE Power & Energy Society General Meeting*, Chicago, IL, Jul. 2017, pp. 1–5, <https://doi.org/10.1109/PESGM.2017.8274468>.
- [12] S. Muchande and S. Thale, "Hierarchical Control of a Low Voltage DC Microgrid with Coordinated Power Management Strategies," *Engineering, Technology & Applied Science Research*, vol. 12, no. 1, pp. 8045–8052, Feb. 2022, <https://doi.org/10.48084/etasr.4625>.
- [13] Y. Wang, T. L. Nguyen, Y. Xu, Z. Li, Q.-T. Tran, and R. Caire, "Cyber-Physical Design and Implementation of Distributed Event-Triggered Secondary Control in Islanded Microgrids," *IEEE Transactions on Industry Applications*, vol. 55, no. 6, pp. 5631–5642, Aug. 2019, <https://doi.org/10.1109/TIA.2019.2936179>.
- [14] A. Bidram, F. L. Lewis, and A. Davoudi, "Distributed Control Systems for Small-Scale Power Networks: Using Multiagent Cooperative Control Theory," *IEEE Control Systems Magazine*, vol. 34, no. 6, pp. 56–77, Sep. 2014, <https://doi.org/10.1109/MCS.2014.2350571>.
- [15] Y. Wang, T. L. Nguyen, Y. Xu, Q. T. Tran, and R. Caire, "Peer-to-Peer Control for Networked Microgrids: Multi-Layer and Multi-Agent Architecture Design," *IEEE Transactions on Smart Grid*, vol. 11, no. 6, pp. 4688–4699, Aug. 2020, <https://doi.org/10.1109/TSG.2020.3006883>.
- [16] Y. Yao and N. Ertugrul, "An Overview of Hierarchical Control Strategies for Microgrids," in *2019 29th Australasian Universities Power Engineering Conference (AUPEC)*, Nadi, Fiji, Nov. 2019, pp. 1–6, <https://doi.org/10.1109/AUPEC48547.2019.211804>.
- [17] M. Liu *et al.*, "A Multi-Agent System Based Hierarchical Control Framework for Microgrids," in *2021 IEEE Power & Energy Society General Meeting (PESGM)*, Washington, DC, USA, Jul. 2021, pp. 01–05, <https://doi.org/10.1109/PESGM46819.2021.9638070>.
- [18] Y. Han, H. Li, P. Shen, E. A. A. Coelho, and J. M. Guerrero, "Review of Active and Reactive Power Sharing Strategies in Hierarchical Controlled Microgrids," *IEEE Transactions on Power Electronics*, vol. 32, no. 3, pp. 2427–2451, Mar. 2017, <https://doi.org/10.1109/TPEL.2016.2569597>.
- [19] M. Maaruf, S. El-Ferik, M. Abido, and M. Khalid, "Two-Loop Distributed Optimal Secondary Voltage Control of an Islanded Microgrid with Multiple Distributed Generators," in *2022 IEEE PES 14th Asia-Pacific Power and Energy Engineering Conference (APPEEC)*, Melbourne, Australia, Nov. 2022, pp. 1–5, <https://doi.org/10.1109/APPEEC53445.2022.10072258>.
- [20] S. Sun, Y. Cheng, D. Wei, and N. Wang, "Management of MicroGrid in Power System in the Perspective of Communication Process of Multi-agent System," *Journal of Physics: Conference Series*, vol. 1815, no. 1, Feb. 2021, Art. no. 012024, <https://doi.org/10.1088/1742-6596/1815/1/012024>.
- [21] J. B. Almada, R. P. S. Leão, R. G. Almeida, and R. F. Sampaio, "Microgrid distributed secondary control and energy management using multi-agent system," *International Transactions on Electrical Energy Systems*, vol. 31, no. 10, 2021, Art. no. e12886, <https://doi.org/10.1002/2050-7038.12886>.